MAGNETIC SYSTEM OF THE TEVATRON ELECTRON LENS (TEL)

Accord
on an Electron Lens Magnet System Design
between the
Fermi National Accelerator Laboratory
(Fermilab)
P.O. Box 500, Batavia, Illinois 60510 U.S.A.
and the
Institute for High Energy Physics (IHEP)
Protvino, Moscow region, 142284, Russia

Report

Bogdanov I.V., Kozub S.S., Pleskach V.V.,
Sytnik V.V., Tkachenko L.M., Zintchenko S.I.,
Zubko V.V.

Abstract

The program of the compensation of beam–beam effects with electron beam on the TEVATRON proton–antiproton collider is being developed in FNAL and it is now under the realization stage. According to this program the determined SC magnetic system should be developed, manufactured, tested and installed in the interaction points of TEVATRON.

In the frame of collaboration between IHEP and FNAL the general drawings of the magnetic system have been developed in IHEP and presented below.

Contents

1 Introduction

In the frames of collaboration between IHEP and FNAL a magnetic system of the Tevatron Electron Lens (TEL) has been developed. TEL is intended for compensation of the beam–beam parasitic effects in the Tevatron with use of high current, low energy electron beam[1].

2 General description of magnetic system

The longitudinal cross-section of the magnetic system of TEL is shown on Fig.1. The magnetic system of TEL consists of a main superconducting (SC) solenoid (2) and two conventional solenoids. An electron gun will be placed in one of the conventional solenoids (1). The second solenoid (3) serves as a part of collector for electron beam. It has more complicate geometry of iron shield with two cylindrical partition divided a collector region from SC and conventional solenoids. The current of the collector solenoid has an opposite sign of SC solenoid. The both solenoids will be installed away from the main proton–antiproton beam.

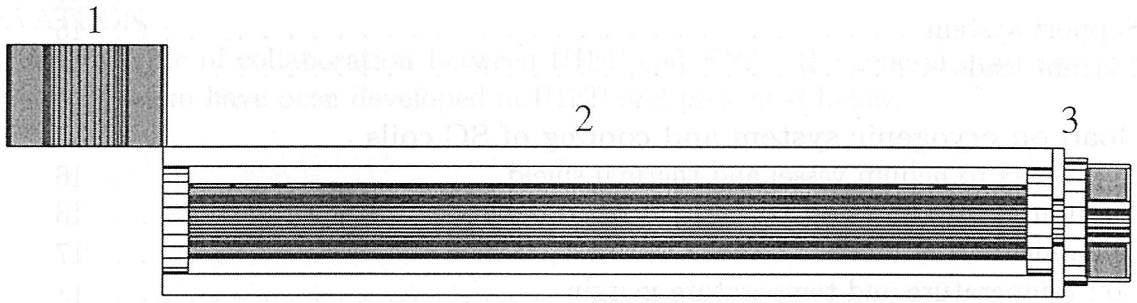

Figure 1: Longitudinal cross-section of the magnetic system of TEL: 1 — electron gun solenoid, 2 — SC solenoid with steering dipoles in the cryostat, 3 — collector.

The SC solenoid will be set up in SC ring of TEVATRON. It provides the electron beam which collides with the antiproton beam. Six steering dipoles are placed on the outer surface of SC solenoid coil. Two pairs of ones are short dipoles on the ends of SC solenoid coil and another pair is long dipoles in central region of SC solenoid. Each pair consists of the vertical and horizontal dipoles. They intend to control the electron beam moving it up–down and left–right.

The electron beam will be born on the electron gun cathode, transported through the interaction region in a strong solenoidal field of the SC solenoid and absorbed in the collector.

3 Computer code for magnetic field calculations

Magnetic field calculations of the magnetic system was carried out using the MULTIC code[2].

The computational algorithm is based on equations to follow.

Magnetic field is decomposed into

$$\vec{B} = \vec{B}_J + \vec{B}_M. \tag{1}$$

Vector $\vec{B}_J$ denotes field due to current in coils found by the Biot-Savart's law:

$$\vec{B}_J(\vec{r}) = \frac{1}{c}\int_{V'} \frac{\vec{J}(\vec{r}) \times (\vec{r} - \vec{r}')}{|\vec{r} - \vec{r}'|^3} dV', \tag{2}$$

which integral can be calculated up to computer precision.

Vector $\vec{B}_M$ is originated by iron with magnetization density vector $\vec{M}$,

$$\vec{B}_M(\vec{r}) = \vec{\nabla}_r \int_{V'} \frac{\vec{J}(\vec{r}) \cdot (\vec{r} - \vec{r}')}{|\vec{r} - \vec{r}'|^3} dV', \tag{3}$$

Finally, the magnetization itself can be found with an integral equation

$$\vec{M}(\vec{r}) = \frac{\mu - 1}{4\pi} \left(\vec{B}_J(\vec{r}) + \vec{\nabla}_r \int_{V'} \frac{\vec{J}(\vec{r}) \cdot (\vec{r} - \vec{r}')}{|\vec{r} - \vec{r}'|^3} dV' \right), \tag{4}$$

This equation is approximated with a non-linear set of algebraic equations solving of which makes the core of numerical algorithm employed. Volume of iron yoke is subdivided into finite elements — triangle prisms and tetrahedrons. Magnetization of each elements is assumed to be constant. Real law $\mu(B)$ of magnetic permeability versus field is taken into account via a scheme of direct iterations.

4 Parameters of SC magnets

The general view of cross section of SC magnets in the first quadrant is shown on Fig.2, where (from center along radius): SC solenoid, horizontal steering dipole, vertical steering dipole, iron.

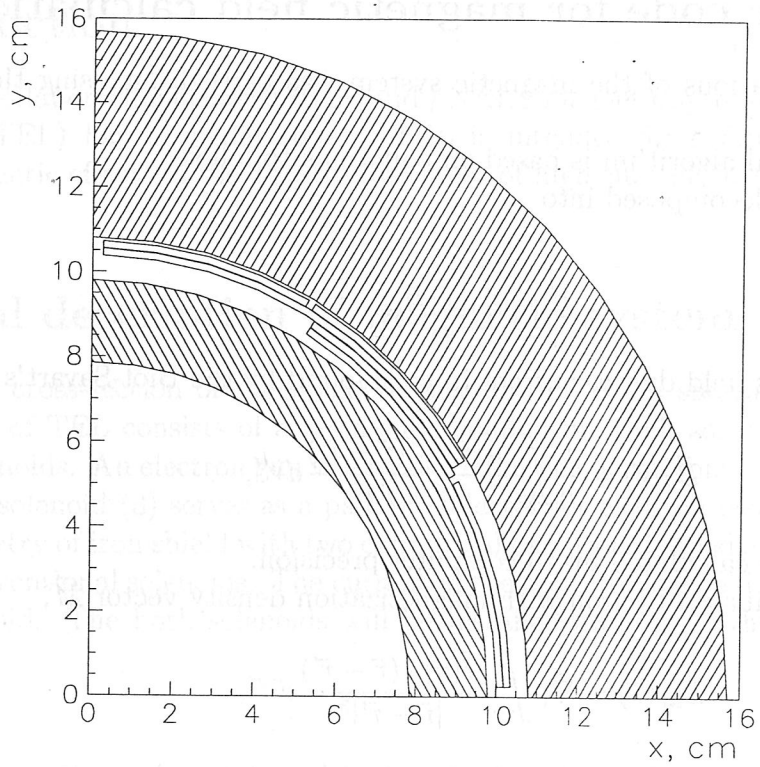

Figure 2: General view of cross section of SC magnets in the first quadrant.

4.1 SC solenoid

The solenoid coil will be manufactured of a flat transposed cable consisting of 10 SC wires each 0.85 mm diameter. The basic characteristics of the SC wire are presented in Table 1.

Table 1: SC wire characteristics for main solenoid.

SC alloy	Nb+50%Ti
Wire diameter, mm	0.85
Number of filament	2970
Filament diameter, μ	10
Twist pitch, mm	10
Matrix material	Cu
Cu/SC ratio	1.38
Critical current at 4.2 K and 5 T, A	540
Critical current density A/cm^2	2.3×10^5

Fig.3 shows the dependence of critical current versus magnetic field at 4.2 K temperature for the SC wire of 0.85 mm diameter.

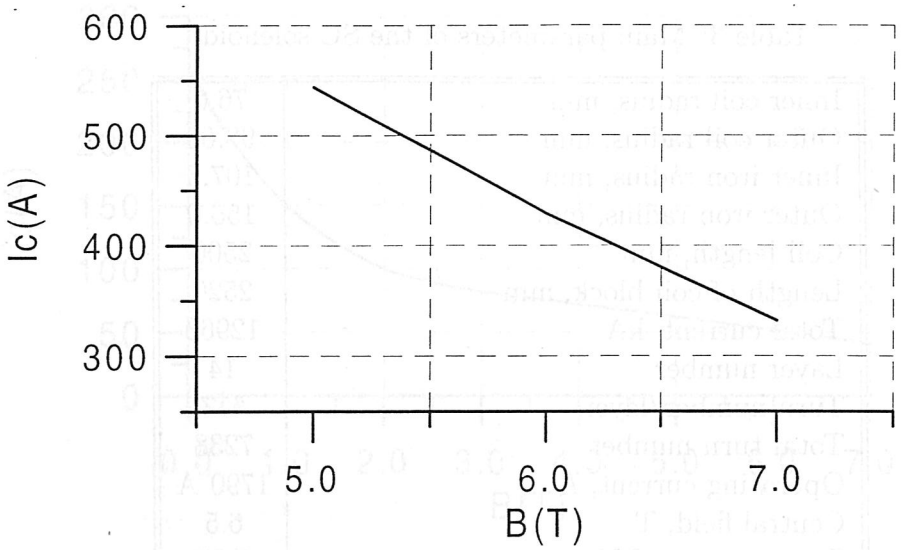

Figure 3: Critical current versus magnetic field at 4.2 K temperature for the SC wire of 0.85 mm diameter.

The main parameters of the current carrying element of SC solenoid are presented in Table 2. Note that the dimensions of cable are defined by using empiric formulae and our production experience. After real manufacture of cable these dimensions will have little deviations. The cable is insulated by three layers of polyimide film.

Table 2: Main parameters of current carrying element of SC solenoid.

Wire number	10
Wire diameter, mm	0.85
Bare dimensions, mm^2	1.44×4.64
Insulation, mm	$3 \times 0.03 = 0.09$
Dimensions with insulation, mm^2	1.62×4.82
Packing factor	0.85

The main parameters of the SC solenoid are presented in Table 3.

Table 3: Main parameters of the SC solenoid

Inner coil radius, mm	76.0
Outer coil radius, mm	98.68
Inner iron radius, mm	107.5
Outer iron radius, mm	156.0
Coil length, mm	2500
Length of coil block, mm	2520
Total current, kA	12963
Layer number	14
Turn number/layer	517
Total turn number	7238
Operating current, A	1790 A
Central field, T	6.5
Stored energy, MJ	0.95
Inductance, H	0.6
Radial pressure, atm	141
Longitudinal forces, tons	39
Operating temperature, K	4.6
Critical current (6.5 T, 4.6 K), A	3000
Critical temperature (6.5 T, 1800 A), K	5.3

The supporting structure for SC coil is the stainless steel tube of $\oslash 152\ mm \times 5.7\ mm$ dimensions. Two flanges with stainless steel are welded together to both edges of tube. The thickness of each flange is 9 mm steel and 1 mm insulation. Both cable ends are left the coil from its outer surface from the one of coil ends. The frame insulation is three layers of polyimide film of 100 μm thickness.

The coil is wound with define tension to provide a necessary radial pressure.

4.2 Steering dipoles

The magnetic system of the steering magnets consists of the lateral and central dipoles (Fig.4). In its turn each of them consists of vertical and horizontal dipoles. In all the total sum of dipoles equals to six. This system allows to move and turn the electron beam in various directions. The steering dipoles are placed on outer surface of solenoid coil (Fig.2).

Figure 4: Longitudinal placement of the steering dipoles.

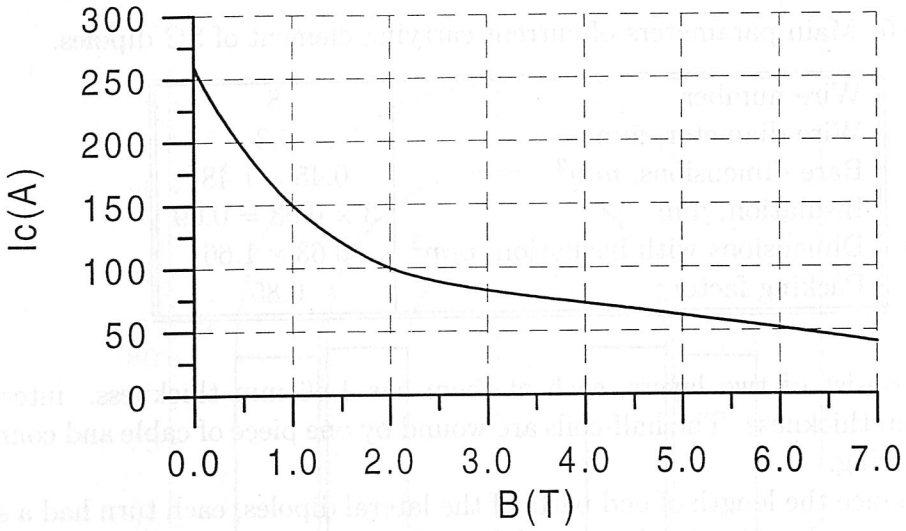

Figure 5: Dependence of critical current on magnetic field at 4.2 K temperature for the SC wire of 0.3 mm diameter.

For design simplification of dipole magnets and reduction of their general cost the coils of all six magnets are wound by the cable with the same dimensions. This is a flat cable transposed from 8 wires of 0.3 mm diameter. The basic characteristics of the SC wire are presented in Table 4.

Table 4: SC wire characteristics for central and lateral dipoles.

SC alloy	Nb+50%Ti
Wire diameter, mm	0.3
Number of filament	150
Filament diameter, μ	15
Twist pitch, mm	25
Matrix material	Cu
Cu/SC ratio	1.5
Critical current at 4.2 K and 5 T, A	≥ 50
Critical current density, A/cm^2	1.8×10^5

Fig.5 shows the dependence of critical current against magnetic field at 4.2 K temperature for the SC wire of 0.3 mm diameter.

The cable has three layers of insulation of polyimide film. For lateral dipoles all wires in cable are SC, currents in central dipoles are essentially less, so the cable for central dipoles has two SC wires and six Cu wires.

The main parameters of the current carrying element of SC dipoles are presented in Table 5.

Table 5: Main parameters of current carrying element of SC dipoles.

Wire number	8
Wire diameter, mm	0.3
Bare dimensions, mm^2	0.45×1.48
Insulation, mm	$3 \times 0.03 = 0.09$
Dimensions with insulation, mm^2	0.63×1.66
Packing factor	0.85

All dipoles consist of two layers, each of them has 1.66 mm thickness. inter–layer spacer has 0.2 mm thickness. The half-coils are wound by one piece of cable and connected together by soldering.

In order to reduce the length of end parts of the lateral dipoles, each turn had a shape, which can be presented in the development (plane $Z - \rho\vartheta$ as two conjugate arcs of small and large radii[3](Fig.6).

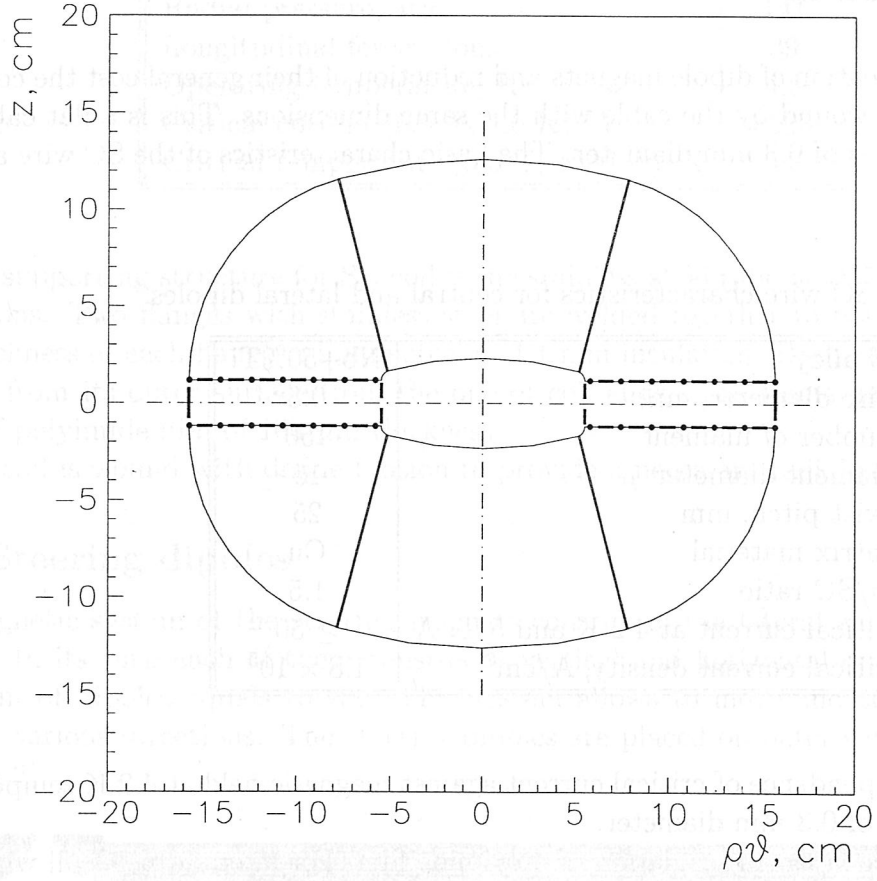

Figure 6: Development of the first layer of lateral horizontal steering dipole.

The central dipoles have an usual shape of end parts as it is shown schematic on Fig.7 for the second layer.

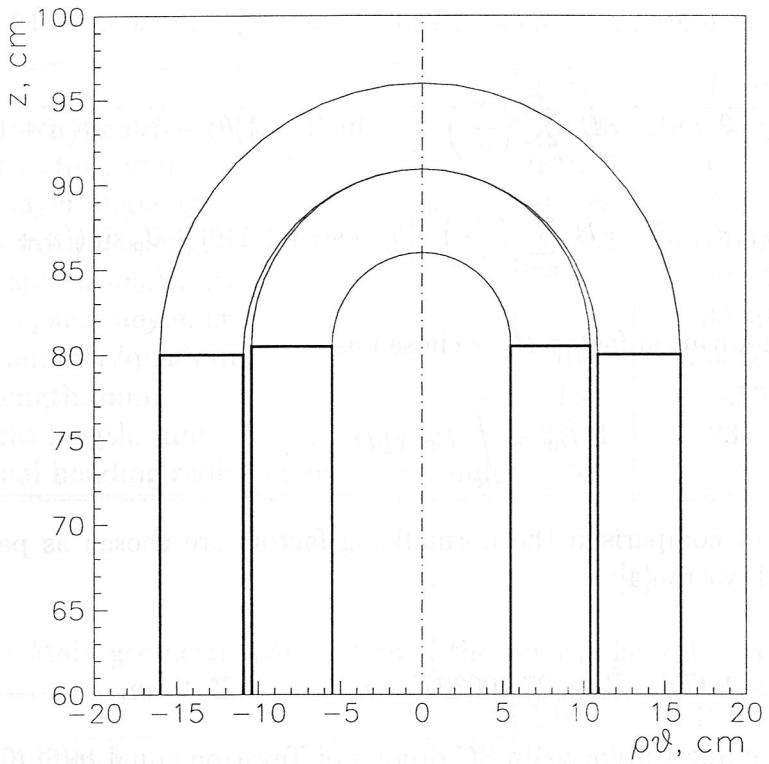

Figure 7: Development of the second layer of central horizontal steering dipole.

4.2.1 Field representation

For multipole magnets components of magnetic field in polar system of coordinates can be presented as a series:

$$B_r(r,\theta) = B_0 \sum_{n=0}^{\infty} \left(\frac{r}{r_0}\right)^n \left[b_n \sin((n+1)\theta) - a_n \cos((n+1)\theta)\right], \tag{5}$$

$$B_\theta(r,\theta) = B_0 \sum_{n=0}^{\infty} \left(\frac{r}{r_0}\right)^n \left[b_n \cos((n+1)\theta) + a_n \sin((n+1)\theta)\right], \tag{6}$$

where B_0 is the normalizing factor, as a rule this is a value of central field, r_0 is the reference radius, b_n and a_n are "normal" and "skew" field nonlinearities of order $n-1$. In ideal dipole magnet only nonlinearities of type $b_{2k}, (k = 1, \ldots, \infty)$ are other than zero. In this case the b_0 nonlinearity is the normalizing dipole field. The nonlinerities of lower orders exert the most influence on beam dynamic. In single layer dipole the b_2 nonlinearity is equals to zero when initial and final layer angles are accordingly: $\phi = \Delta, \alpha = 60° - \Delta$.In order to match the angle extent of the outer layer to the inner one, the inter-turn spacer are inserted in the second layer in position $(30° - \delta, 30° + \delta)$.

One can get the expansion of the integral field similar to (1)–(2):

$$\hat{B}_r(r,\theta) = \int_{-\infty}^{\infty} B_r(r,\theta,z)dz = \hat{B}_0 \sum_{n=0}^{\infty} \left(\frac{r}{r_0}\right)^n \left[\hat{b}_n \sin((n+1)\theta) - \hat{a}_n \cos((n+1)\theta)\right], \quad (7)$$

$$\hat{B}_\theta(r,\theta) = \int_{-\infty}^{\infty} B_\theta(r,\theta,z)dz = \hat{B}_0 \sum_{n=0}^{\infty} \left(\frac{r}{r_0}\right)^n \left[\hat{b}_n \cos((n+1)\theta) + \hat{a}_n \sin((n+1)\theta)\right], \quad (8)$$

Usually the normalization factor $\hat{B}_0$ is chosen as

$$\hat{B}_0 = \int_{-\infty}^{\infty} B_0(z)dz. \quad (9)$$

For convenience of comparison the normalizing factors are chosen as parameters of main SC dipoles of Tevatron[4]:

$$B_0 = 4.4T; \quad \hat{B}_0 = 27.70632T \times m; \quad r_0 = 25.4mm.$$

Note the lower nonlinerities of main SC dipoles of Tevatron equal to[5] (Table 6):

Table 6: Values of the lower nonlinerities b_n of main SC dipoles, 10^{-4}.

n	Design	Mean	RMS
2	0.04	0.95	3.12
4	1.04	-0.57	1.32
6	4.44	5.48	0.54
8	-12.09	-12.52	0.33
10	3.63	3.70	0.26

Both the field and integral field nonlinearities were calculated with help of code HARM-3D[6].

4.2.2 Lateral dipoles

The main geometric parameters of the horizontal (inner) and vertical (outer) lateral SC steering magnets are presented in Tables 7 and 8.

Table 7: Main geometric parameters of the horizontal lateral SC dipoles.

	I layer	II layer
Inner radius, mm	100.08	101.84
Outer radius, mm	101.74	103.50
Inner layer angle, gr.	1.389	1.366
Outer layer angle, gr.	58.555	58.555
Inner spacer angle, gr.	–	29.459
Outer spacer angle, gr.	–	30.462
Turn number/quadrant	160	$160 = 80 + 80$
Coil length, mm	250	250
Straight length, mm	23.34	23.34
Minimal bending radius of end parts, mm	5	5

Table 8: Main geometric parameters of the vertical lateral SC dipoles.

	I layer	II layer
Inner radius, mm	103.70	105.46
Outer radius, mm	105.36	107.12
Inner layer angle, mm	2.45	2.50
Inner layer angle, gr.	1.369	1.346
Outer layer angle, gr.	58.626	58.626
Inner spacer angle, gr.	–	29.501
Outer spacer angle, gr.	–	30.471
Turn number/quadrant	164	$166 = 83 + 83$
Coil length, mm	250	250
Straight length, mm	15.2	18.6
Minimal bending radius of end parts, mm	5	5

The main magnetic parameters of the lateral dipoles are presented in Table 9.

Table 9: Main magnetic parameters of the lateral SC dipoles.

	Horizontal	Vertical
Total maximal current/coil, kA	64.0	66.4
Maximal turn current, A	200	200
Current density, A/mm^2	191	191
Central field, T	0.7888	0.8169
Integral field, $T \times m$	0.123	0.138
Magnetic length, m	0.1424	0.1394
Stored energy, kJ	1.15	1.31
Inductance, mH	57	66
Operating temperature, K	4.6	4.6
Critical current (2.2 T, 4.6 K), A	640	640
Critical temperature (2.2 T, 200 A), K	7.1	7.1
$b_2 \times 10^{-4}$	0.14	0.04
$b_4 \times 10^{-4}$	-1.40	-1.39
$\hat{b}_2 \times 10^{-4}$	-0.19	-0.21
$\hat{b}_4 \times 10^{-4}$	-0.03	-0.03
Ponderomotive forces/quadrant		
F_x, kN	4.68	5.10
F_y, kN	-0.91	-0.78
$\|F\|$, kN	4.77	5.15

The nonlinearities of higher orders both central and integral field are negligible.

4.2.3 Central dipoles

The geometry of the cross-section of the central SC steering magnets are the same as the geometry of the cross-section of the lateral SC steering magnets. The total lengths of the vertical and horizontal dipoles equal to 1940 mm and the straight parts equal to 1713.3 mm and 1705.3 mm accordingly. The rest magnetic parameters are presented in Table 10.

Table 10: Main magnetic parameters of the central SC dipoles.

	Horizontal	Vertical
Total maximal current/coil, kA	16.0	16.6
Maximal turn current, A	50	50
Current density, A/mm^2	48	48
Central field, T	0.1972	0.2042
Integral field, $T \times m$	0.361	0.374
Magnetic length, m	1.8324	1.8294
Stored energy, kJ	0.93	1.07
Inductance, H	0.74	0.86
Operating temperature, K	4.6	4.6
Critical current (0.5 T, 4.6 K), A	360	360
Critical temperature (0.5 T, 50 A), K	8.3	8.3
$b_2 \times 10^{-4}$	0.14	0.04
$b_4 \times 10^{-4}$	-1.40	-1.39
$\hat{b}_2 \times 10^{-4}$	-0.16	-0.20
$\hat{b}_4 \times 10^{-4}$	-0.41	-0.41
Ponderomotive forces/quadrant		
F_x, kN	3.77	4.18
F_y, kN	-0.73	-0.64
$\|F\|$, kN	3.84	4.23

The nonlinearities of higher orders both central and integral field are also negligible.

4.3 Magnetic shield

SC solenoid coil together with steering dipoles are enclosed in magnetic iron with inner radius of 107.5 mm and 48.5 mm thickness. The yoke reduces currents in steering coils, improves field inhomogeneity inside solenoid aperture, condensates magnetic force lines on ends of coil block and shields external space from magnetic field. The iron is cold and it is placed into cryostat. The yoke will be produced with low-carbon steel of quality like CT2081. This steel was used at manufacturing of pilot industrial batch's of SC dipole for UNK[7], which possessed a high field quality. The characteristics of this steel were measured very well under cryogenic temperature and in wide field range.

The yoke will be produced with four non-laminar blocks of 2500 mm length and fixed by studs. The outer surface of iron has 24 grooves with width of 20 mm and depth of 3.5 mm. The grooves serve for passage of helium flow and they are also used for laying of cables for central and lateral dipoles.

The yoke is tightened by two stainless steel half-shells of 5 mm thickness after that the shells are welded. The half-shells serve as an outer shell of helium vessel and they give a stiffness of all assembly of SC coil block.

5 Cryostat

The cryostat consists of the main following units:

- helium vessel;
- thermal shield;
- vacuum vessel;
- support system of cold mass;
- current leads.

5.1 Helium vessel

The block of SC solenoid and six steering dipoles together with magnetic iron are enclosed in helium vessel. The vessel has $\oslash 151.4\ mm \times 5.7\ mm$ inner tube, $\oslash 324\ mm \times 6\ mm$ outer shell and 2590 mm length. The shell of vessel supplies stiffness of the coil block. The buckling of the vessel is less than 0.01 mm. Besides the shell creates preload of SC coils to supply necessary mechanical stress in the coil during mode of operation.

There is a box in the head part of helium vessel. The box contains current leads and branch pipes for helium input and emergency dump.

Liquid helium cools SC coils in the vessel and returns from the back part of the vessel through the tube of 20 mm inner diameter.

5.2 Thermal shield

The parts of the shield are manufactured of 2 mm thick copper sheet. The main part of the shield is suspended on the titanium rods and the suspension points work like heat intercepts.

The outer surface of the shield is covered with 40 layers of superinsulation. The front walls of the shield and the inner tube are welded after adjustment of the helium vessel position relatively to the vacuum vessel and referencing solenoid axis to the reference points.

The shield is cooled by nitrogen boiling flow passing through the 14 mm inner diameter tube brazed to the main part of the shield. The nitrogen flow returns to the string trough the similar tube which has no thermal contact with the shield.

Small radial gap between the 300 K tube and the 80 K inner copper tube do not allow to cover the inner stainless steel tube with superinsulation. It will be covered with several layers of the aluminized PET film to provide low surface emissivity. Radiation heat leak to the inner copper tube is estimated as 7.5 W, and the temperature in the middle of the tube is 12 K higher than at the tube ends.

Temperature difference along the radius of the front plate is about 1 K. Heat leaks to the main shell of the shield are estimated as 3.5 W through the superinsulation and

8.5 W along the supports. Heat interceptions of the safety valve tube and of the copper voltage taps add about 1 W and 1.5 W respectively. The maximum temperature of the main shell is about 2 K higher than that of liquid nitrogen. Total heat load at 80 K is about 25 W including 3 W from two bayonet joints.

5.3 Vacuum vessel

The vacuum vessel is made from stainless steel and its main part serves as a frame for cold mass. The vessel has $\oslash 114\ mm \times 2.1\ mm$ inner tube, $\oslash 480\ mm \times 5\ mm$ outer shell and 2690 mm length. The tension members of cold mass, a valve for vacuum evacuation, platforms for construction ball, support brackets as well as bosses with holes for transport bolts are welded to the main part.

There are two boxes in the head part of the vacuum vessel. Former box contains current leads, units of helium input–output, emergency dump, connectors of potential wires. The latter has unit of nitrogen input–output.

8 ml/s air must be put on the blow in annular gap between vessel inner tube and collector tube to keep inner tube wall at room temperature.

5.4 Support system

The cold part of the magnetic system with mass of about 1350 kg is hung up to the vacuum vessel in two cross-sections with help of two vertical suspensions and two horizontal tension members in each of cross-sections.

For ease of cryostat assembly each of supports consists of nitrogen and helium parts. The both parts are fixed to nitrogen shield by threaded connection. The tension members are made of titanium alloy and have diameter of 10 mm. The support system allows to withstand the overload not less than 1 g.

The location of the helium vessel and shield connected with helium vessel are adjusted along horizontal and vertical directions by help of spherical nuts which are carried by washers.

In the axial direction the cold mass is fixed by help of longitudinal titanium tension members and anchor fixed on vacuum vessel.

5.5 Current leads

The current leads of the main solenoid are calculated on the current of 1800 A. The current leads are a braid of 3500 cooper wires of 0.13 mm diameter.

The braid is placed in stainless tube of $\oslash 16\ mm \times 1\ mm$. Glass-cloth-base laminate tube of $\oslash 14\ mm \times 1\ mm$ is between cooper wires and stainless tube as electrical insulation. The current lead is cooled by helium vapour and helium flow equals to 92 mg/s. The pressure drop of the flow is 6000 Pa. The cooled part length is about 750 mm. Heat leak through current lead to liquid helium is equal to 2 W.

The current leads of the dipole magnets are calculated on the current of 200 A. The cooper tube of $\oslash 8\ mm$ is a current carrying element. Six tubes are connected by glass-cloth-base laminate washers in assembly. The washers are pulled on the tubes and are glued between themselves. The assembly is placed in $\oslash 40\ mm \times 1\ mm$ stainless tube. The washers have spacial groove and holes for 65 mg/s cooling helium gas flow. The pressure drop of the gas flow is equal to 30000 Pa. Heat leak through current lead to liquid helium is 1.4 W.

Two such assemblies are provided power of the six dipoles.

6 Heat load on cryogenic system and cooling of SC coils

6.1 Heat leaks to helium vessel and thermal shield

The heat leak budget at 4.6 K and 80 K is presented in Table 11:

Table 11: Budget of heat leaks, W.

	4.6 K	80 K
Radiation	0.2	11
Supports	1.2	8.5
Safety valve	0.5	1.0
Current leads of SC solenoid	4.0	
Current leads of dipoles	2.8	
Voltage taps	0.5	1.5
Two bayonet joints	3.0	3.0
Total	12.2	25.0

The consumption of liquid helium for cooling of current leads is 5.2 l/hr for SC solenoid and 3.8 l/hr for SC dipoles.

6.2 Helium flow pressure drop

Cryostat is a part of the TEVATRON magnet string. So 24 g/s of liquid helium pass through the helium vessel of the TEL cryostat. There are 24 channels in the yoke to cool the SC solenoid and dipole magnets.

Pressure drop in the channels was estimated as 30 Pa assuming reasonable walls roughness and taking into account local pressure drops due to the change of the cross section.

The tube of 20 mm I.D. is used to return helium flow to the string and it adds about 35 Pa of pressure drop.

Total pressure drop does not exceed 100 Pa.

There is no two phase helium cooling in the TEL cryostat and the temperature of helium leaving cryostat will be 0.1 K higher than inlet temperature.

6.3 Dynamic heat release at the SC solenoid excitation

During the change of current through the SC solenoid heat release occurs in coil and other metal parts. There are two type of heat losses. The one of them is determined by hysteresis character of magnetization of superconductor and electrical steel of yoke. The other is provoked by eddy currents generated in inner stainless pipe, into the copper matrix of SC wires and in the yoke.

At the heat losses estimations the results of early made measurements of properties of structural materials and superconductor[8, 9] were used. The results of calculation of heat release power for the main components of SC solenoid design are summarized in Table 12.

Table 12: Power of dynamic heat releases in the SC solenoid, W.

	Current ramp rate, A/s		
	18	4.5	1.125
Heat losses in coil			
Hysteresis component	4.5	1.13	0.28
Matrix component	0.1	0.006	—
Total in coil	4.6	1.14	0.28
Heat losses in other metal parts			
Inner pipe	0.15	0.009	—
Yoke (eddy current, flux change in bore)	1.55	0.1	0.06
Yoke (eddy current, iron magnetization)	1.85	0.12	0.007
Yoke (hysteresis)	0.13	0.03	0.008
Total in iron	3.68	0.26	0.075
Total heat release power in SC solenoid	8.38	1.4	0.36

Table 12 presents the power averaged for full cycle of SC solenoid excitation, when current is changed from zero up to its nominal value and inversely down to zero at three values of current ramp rate. From this Table it is obvious that in the coil the hysteresis losses in superconductor are significantly prevalent over matrix losses, whereas a cable losses are absent. In the other main metal parts the eddy current losses in the yoke are predominant.

The dependences of heat release power in coil, metal parts and summary power versus current rump rate are shown on Fig.8. It is clearly noticeable from this figure that the current ramp rate less than 5 A/s is quite suitable for magnet excitation.

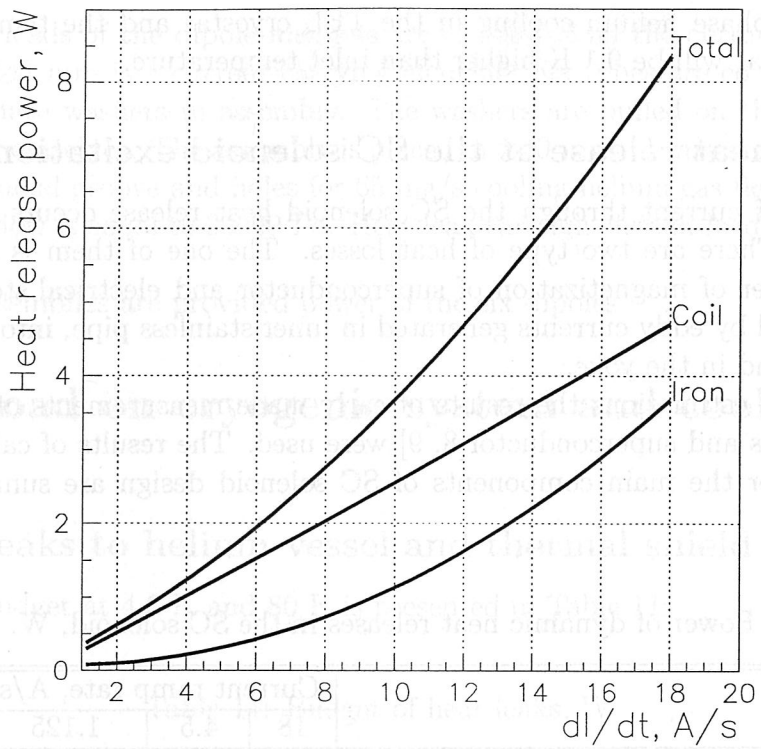

Figure 8: Dependences of heat release power in coil, metal parts and summary power versus current rump rate.

6.4 Coil temperature and temperature margin

TEL SC coils are not "dry", they contain about 15% of liquid helium by volume. But there is no organized cooling flow inside the coils. Cooling channels are cut on the outer surface of the iron yoke. Therefore inner most turns of the solenoid will have the highest temperature and the same turns will be in the highest field.

Polyimide insulation presents main barrier for the heat flux in radial direction. Considering the coil as a "dry" multilayer cylinder and assuming the heat conductance of the superconductor infinitely high comparing with that of the polyimide one can get 0.07 W/m/K as the effective thermal conductivity of this sandwich at 4.5 K.

To close the thermal circuit it is necessary to take into account the thermal resistance of the bulk cold iron having thermal conductivity about 1 W/m/K.

In the normal mode of operation only 0.05 W of the heat leak from the inner copper tube (thermal shield) are to be transferred to the helium channels giving a 0.01 K increase in the coil temperature. In the previous paragraph the current ramp rate less than 5 A/s was chosen to satisfy the Technical Specification limit of 15 W total heat load at 4.5 K. It results in about 1.4 W approximately evenly distributed in the volume of the coil. Calculated temperature rise of the inner most turns is 0.29 K.

In the worst case the superposition of all three effects gives the cable temperature rise:

heating up of cooling flow	0.1 K
static temperature rise	0.01 K
dynamic temperature rise	0.29 K
heating of inner layer in SC solenoid	0.4 K

The linear dependence of the critical temperature on current can be used to estimate critical temperature for inner layer turns of the SC coil at nominal magnetic field:

$$T_c(B,I) = T_c(B,0) - [T_c(B,0) - 4.2]\frac{I}{I_c(B,4.2)}, \tag{10}$$

where I is coil current, B is magnetic field in coil point, $I_c(B,4.2)$ is the critical current of cable at B and 4.2 K, $T_c(B,0)$ is the critical temperature at B and $I = 0$:

$$T_c(B,0) = T_{c0}(1 - B/B_{c0})^{0.65} = 9.2(1 - B/14.5)^{0.65}. \tag{11}$$

The main results of calculation are presented in Table 13, where $T_0 = T_c(B,0)$, $T = T_c(B,I)$, $\Delta T = T_c(B,0) - 4.2$, $I_c = I_c(B,4.2)$.

Table 13: Critical temperature of SC coils.

SC coil	I, A	B, T	I_c, A	T_0, K	T, K	ΔT, K
Main solenoid	1800	6.5	3800	6.3	5.3	0.7
Lateral dipole	200	2.2	720	8.2	7.1	2.5
Central dipole	50	0.5	400	8.9	8.3	3.7

The minimal difference between critical temperature and liquid helium temperature (4.6 K) is 0.7 K in inner wire of SC solenoid coil. Its temperature margin is 0.3 K at current input and 0.6 K at $I = 1800\ A = const$.

7 Quench behaviour and protection.

7.1 Main SC solenoid.

The stored energy in main SC solenoid is rather big: about 1 MJ. The studying of behaviour during transition to the resistive state (quench) shows that the main solenoid coil is not self-protected against resistive transition and quench should threaten the integrity of the main solenoid. Thus some protective precautions namely, fast quench detection and removal of stored energy to the external dump resistor, must be taken.

Appearance of normal zone in coil is detected by quench detector. Preliminary studies showed that the bridge type of quench detector is most suitable such as the other techniques of compensation of coil inductive voltage are more challenging due to low value of

current ramp rate. When the resistive part of voltage exceeds of given threshold by the amplitude and by time, the dump resistor Rd is turned on by switch S2 and power supply is switched off by S1. Sketch of assumed protection method is shown in Fig.9. Maximum voltage during the energy extraction was accepted from the point of view of insulation reliability and it is equal to 1000 V when $Rd = 0.56$ Ohm. SCR should be used as switch S1 and diodes for switch on the dump resistor. The weight of dump resistor is 26 kg, its temperature rise during energy extraction does not exceed 80 K.

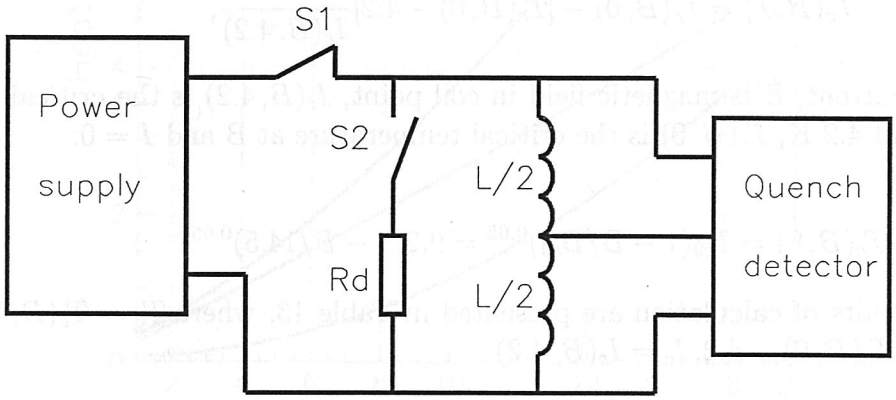

Figure 9: Sketch of protection method.

Simulation of quench spread through the coil was made for the case when quench was provoked on the one side of inner layer of coil, the quench detector threshold $Ut = 1$ V, time delay $Td = 50$ ms and energy discharges on dump resistor $Rd = 0.56$ Ohm. Results are presented on Fig.10. The time dependences of normal zone velocity, current, dump resistor and coil voltage, energy dissipated in coil and dump resistor, and hot spot temperature are shown on picture. It is evident from this curves that almost 90% of stored energy is dissipated outside of cryostat. Amount of energy liberated in coil is sufficient for adiabatic heating of the whole coil up to 80 K. But coil is heated nonuniformly and maximum temperature of coil hot spot reaches 270 K. Temperature profiles of heated region along inner and outer layers of solenoid coil are shown on Fig.11.

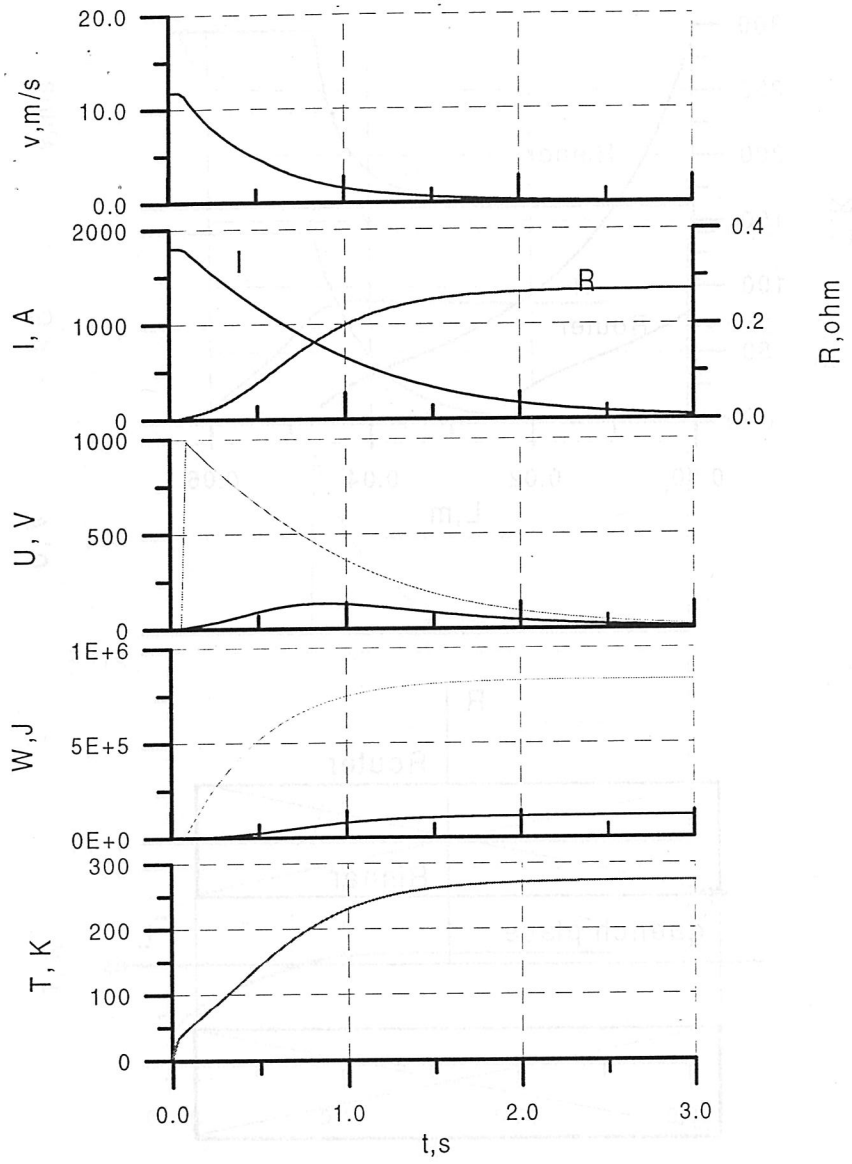

Figure 10: Quench process in main SC solenoid.

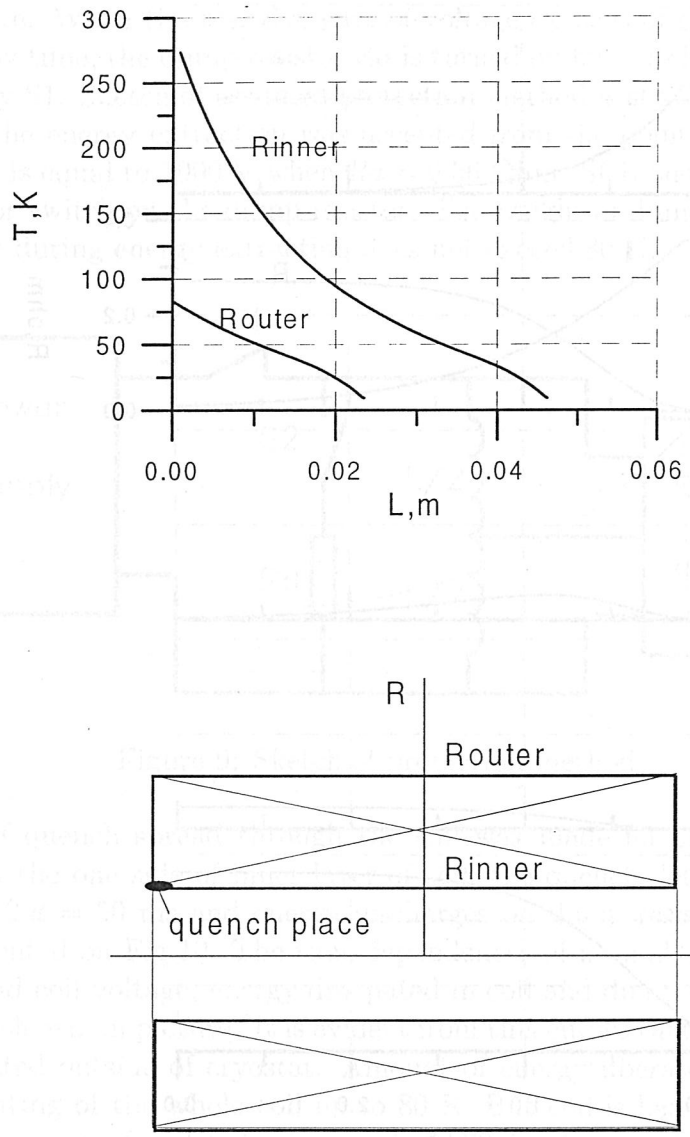

Figure 11: Coil temperature profile in SC solenoid after quench.

7.2 Lateral and central SC steering dipoles.

The energy stored in coils is about 1.3 kJ. The results of simulation of quench process in the coils show that, in essence, after detection the quench and switch off the current supply one can allow all the energy to be dissipated in the coil.

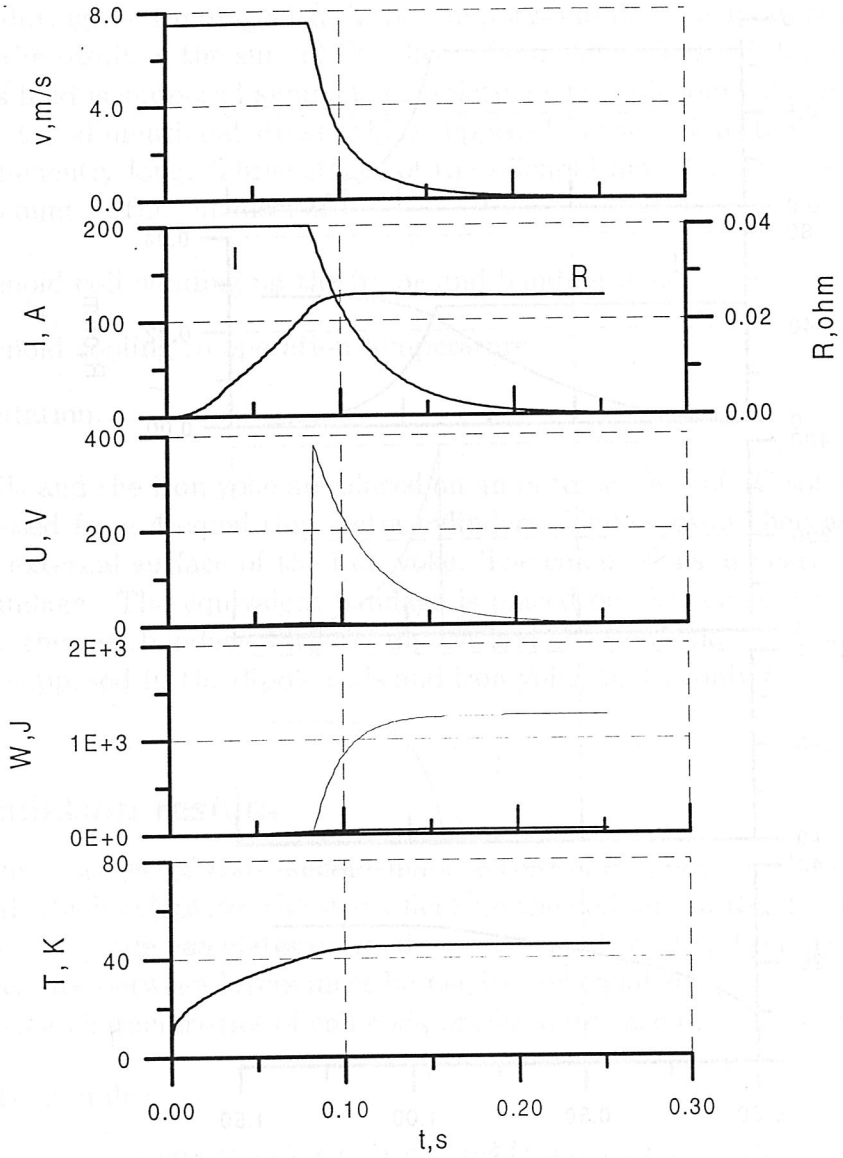

Figure 12: Quench process in lateral SC dipole.

In this case coil hot spot temperature will be about 120 K at lateral dipoles and 50 K at central dipoles. But if it is desirable to lower this temperature in order to reduce the possibility to spread the quench to main solenoid, the same scheme of quench protection as for main solenoid should be used. The results of simulation of quench processes in lateral and central dipoles are presented in Fig.12 and Fig.13. Maximum voltage on the resistor is 400 V (the value of resistance is 2 Ohm for lateral and 8 Ohm for central dipoles), the maximum resistor's temperature rise 80 K. In this case hot spot temperature does not exceed 43 K for lateral and 29 K for central dipoles. Mechanical switches should be used as switch S1 and S2.

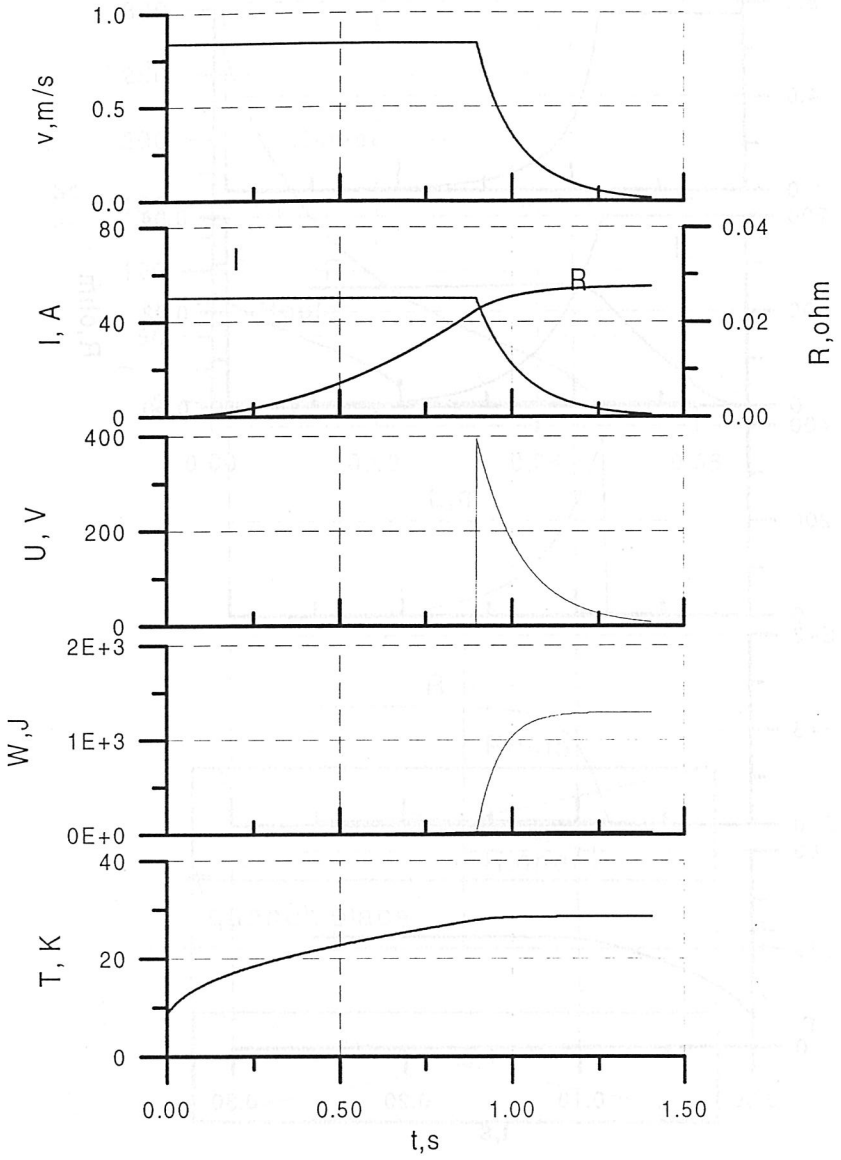

Figure 13: Quench process in central SC dipole.

8 Mechanical stress in main solenoid

8.1 Choice of calculation method

Movements of SC wires cause degradation and training in the SC coils. The winding of solenoid with the preliminary tension allows to reduce this undesirable phenomenon.

The used method of coil stress calculations during all stages of manufacture and operation is described in [10].

The solenoid coil is the anisotropic elastic medium, in which tangential and radial

stresses arise during the winding with the preliminary tension. The final stress distribution in the coil is the result of the sum of the effects from the various coil layers action.

The stress field is supposed symmetrical relatively the solenoid axis and the center of solenoid. The two-dimensional stress field is supposed in the coil, as the relative length of the coil is sufficiently long. Three stages of the solenoid manufacture and operation are taken into account in the calculations:

- the solenoid coil winding on the frame and banding of coil;
- the solenoid cooling to operation temperature;
- coil excitation.

Dipole coils and the iron yoke are placed on an outer surface of SC solenoid. The iron yoke is composed from 4 equal ring sector cylinders. The cryostat shell as a bandage is placed on an external surface of the iron yoke. The calculations are carried out with an equivalent bandage. The equivalent bandage is placed on the solenoid coil and has the same effect as the real bandage with SC dipoles and the iron yoke. The one-dimensional stress field is supposed in the dipole coils and iron yoke, that is only radial stresses cause deformation.

8.2 Calculation results

To analyze three stages of the solenoid manufacture and operation the computer code was developed which calculates the stress fields in the coil and in the design elements on coil boundary. The code calculates optimal parameters of winding keeping the continuity condition: pressure between layers must be positive or equal zero.

The following characteristics of coil components were taken in calculations[11]:

- elasticity modules:
  - insulation at 300 K and 4 K: 1.5×10^4, $1.0 \times 10^5 kgf/cm^2$;
  - conductor at 300 K and 4 K: 2.8×10^5, $3.0 \times 10^5 kgf/cm^2$;
  - cryostat shell, frame and iron yoke: $2.0 \times 10^6 kgf/cm^2$
- Puasson's factor: 0.33;
- coefficient of thermal expansion:
  - insulation: -1.0×10^{-2};
  - conductor: -2.8×10^{-3} ;
  - frame and cryostat shell: -3.0×10^{-3};
  - iron yoke: -2.1×10^{-3}.

Preliminary calculations showed, that pressures acting on the frame and bandage decrease together with reduction of their thickness. On the other hand the strength of both frame and bandage demand to increase their thickness. This compromise causes additional difficulties in the choose of the optimal parameters of solenoid.

Pressure (P), tangential stress (σ) and radial movement (u) in layers of main solenoid at stages 1, 2, 3 accordingly are presented in Table 14.

Table 14: Pressure (kgf/cm^2), tangential stress (kgf/cm^2) and radial movement (μm) in layers in SC solenoid.

	Preload			After cooling			1800 A current		
r, mm	P_1	σ_1	u_1	P_2	σ_2	u_2	P_3	σ_3	u_3
6.1	113	298	102	99	256	-146	0.2	459	-99
77.6	105	302	104	91	257	-149	13	450	-102
79.3	96	307	107	84	259	-153	25	443	-105
80.9	88	312	110	77	261	-155	36	436	-108
82.5	80	318	113	70	265	-158	44	431	-111
84.1	73	324	117	64	269	-161	51	427	-114
85.7	65	331	121	57	273	-163	57	424	-116
87.4	58	338	126	51	278	-165	61	422	-118
89.0	50	346	129	45	284	-166	63	421	-121
90.6	43	354	133	39	290	-168	64	421	-122
92.2	36	363	138	33	296	-169	63	422	-124
93.8	30	372	143	27	303	-170	60	424	-126
95.5	22	381	148	22	310	-171	56	427	-127
97.1	16	390	153	16	317	-172	51	431	-128
98.7	9	399	158	11	324	-173	44	435	-129

The tension in cable is equal to 415 kgf/cm^2 during coil winding.

The iron yoke must transfer only the radial stresses. Therefore azimuthal clearance not less than 0.2 mm between each of separate parts of iron yoke during assembling must be done.

In operation conditions the quench can arise in main solenoid. In this case the helium pressure can increase to 20 kgf/cm^2. The pressure acting on the frame (see Table 14) is equal to 119 kgf/cm^2. The pressure acting on cryostat shell is calculated as pressure acting at stage 3 multiplied by the external solenoid coil radius and divided by the internal shell radius. Accordingly this pressure is equal to 28 kgf/cm^2. Total pressure is equal to 48 kgf/cm^2 at quench.

9 Conventional solenoids

The main parameters of the current carrying element for both conventional solenoids are presented in Table 15.

Table 15: Main parameters of current carrying element of conventional solenoids.

Conductor material	Cu
Insulation material	glass tape
Bare dimensions, mm^2	8.25×8.25
Diameter of water hole, mm	4.6
Insulation, mm	$2 \times 0.2 = 0.4$
Dimensions with insulation, mm^2	9.05×9.05

Electric insulation of bus bar consists of two layers of glass tape.

9.1 Electron gun solenoid

The main parameters of the solenoid for electron gun are presented in Table 16.

Table 16: Main parameters of electron gun solenoid.

Inner radius, mm	125
Outer radius, mm	237
Length, mm	300
Turn number	375
Layer number	12
Maximal total current, kA	134
Maximal operating current, A	357
Maximal central field, T	0.4
Number of cooling circuits	6
Total water flow, kg/s	0.16
$\Delta T,^\circ C$	30
Water Δp, atm	6.8

The stainless steel tube with outer diameter of 247 mm serves as a frame for coil winding. The tube is wound by glass tape impregnated by epoxy compound. After polymerization of compound the tube is treated to diameter of 250 mm.

The coil is divided by six sections. All sections have electric series connection and parallel water connection. The connections are performed by help of commutating units.

The outer surface of coil is insulated by two layers of glass tape. The coil as a unit is impregnated by special compound on the base of epoxy resin.

Two cheeks are installed on the ends of the frame tube with distance of 300 mm. The cheeks are fixed to the frame tube by keys placed in grooves of cheeks and cutting of tube.

There are four reference points and two support brackets on the cheeks.

Electron gun solenoid has an iron frame with thickness of 10 mm to shield an external space from magnetic field.

The general fiew of the electron gun solenoid is shown on Fig.14. The solenoid coil consists of the 17 pairs of cooper "pancakes". Each pair is wound with one whole piece of cable. The winding is started from the center of cable and both ends of cable is created each "pancake".

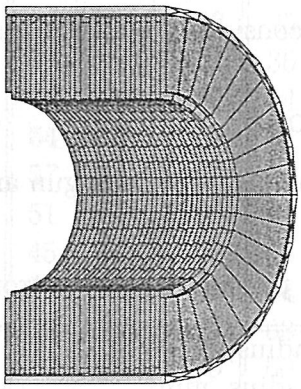

Figure 14: General view of the electron gun solenoid.

In spite of the comb into the inner and outer surfaces of the coil, the magnetic force lines are smooth (Fig.15).

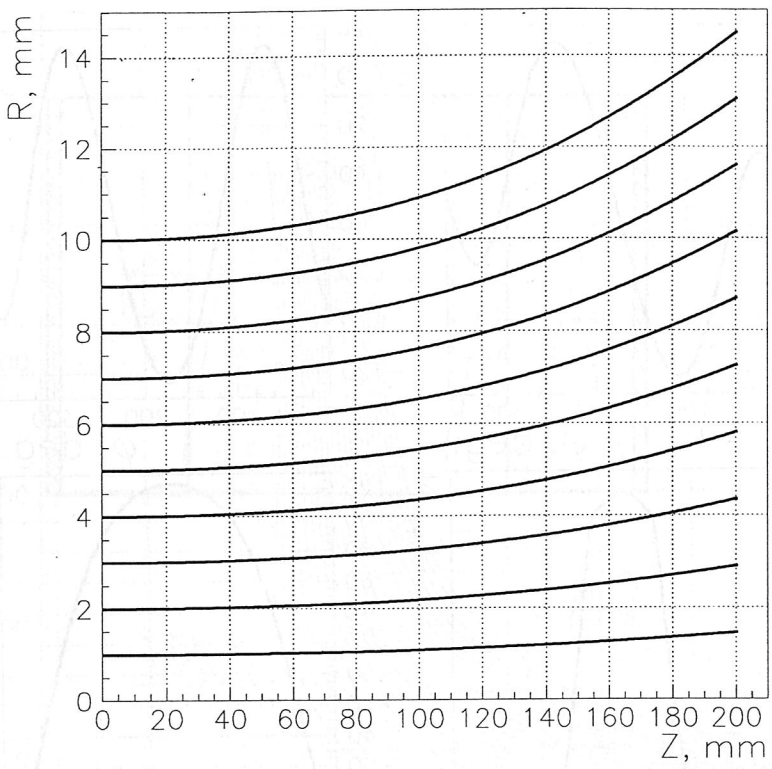

Figure 15: Magnetic force lines along axis of electron gun solenoid.

The distribution of the ponderomotive force components acting to the electron gun solenoid in assembly with SC solenoid is shown on Fig.16 versus azimuthal angle in coordinate system of electron gun solenoid. Angle reading is from farthest point from SC solenoid. Resultant forces equal to 1.853 kN in perpendicular direction to the axis of SC solenoid and 8.472 kN in parallel direction. The total force equals to 8.675 kN.

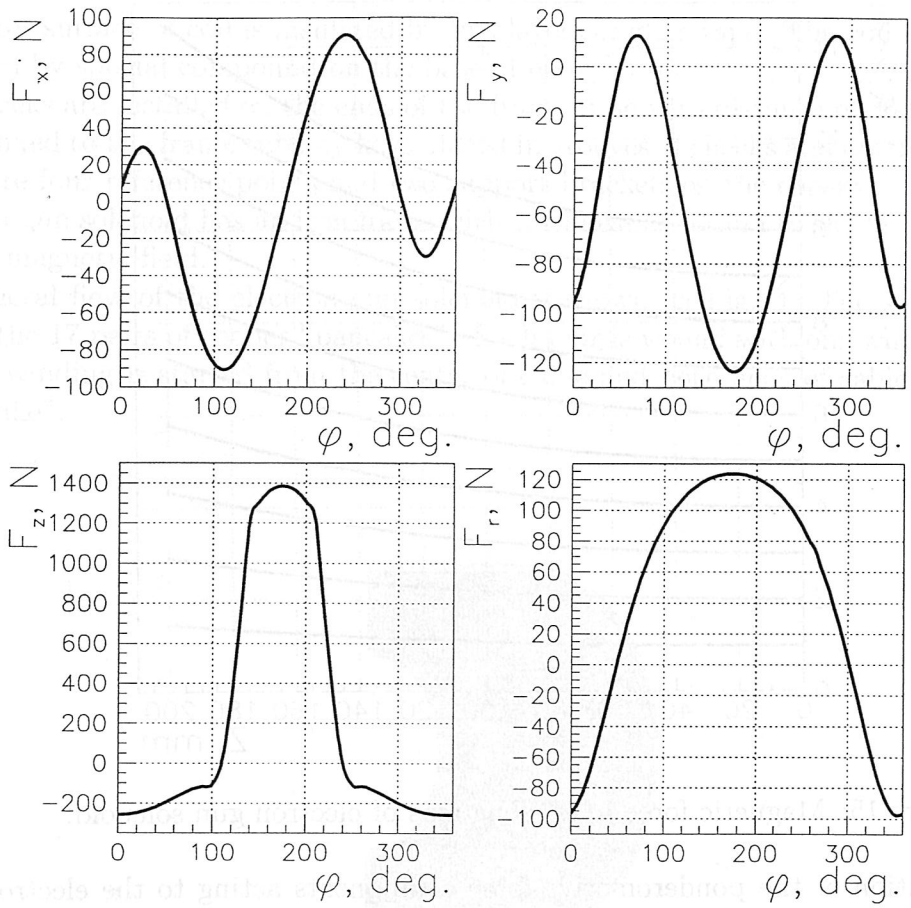

Figure 16: Ponderomotive forces having effect on the gun solenoid against azimuthal angle.

The magnetic force lines from electron gun solenoid to SC solenoid are shown on Fig.17. These lines go through the center of SC solenoid in radial direction from -10 mm to $+10$ mm with step of 1 mm.

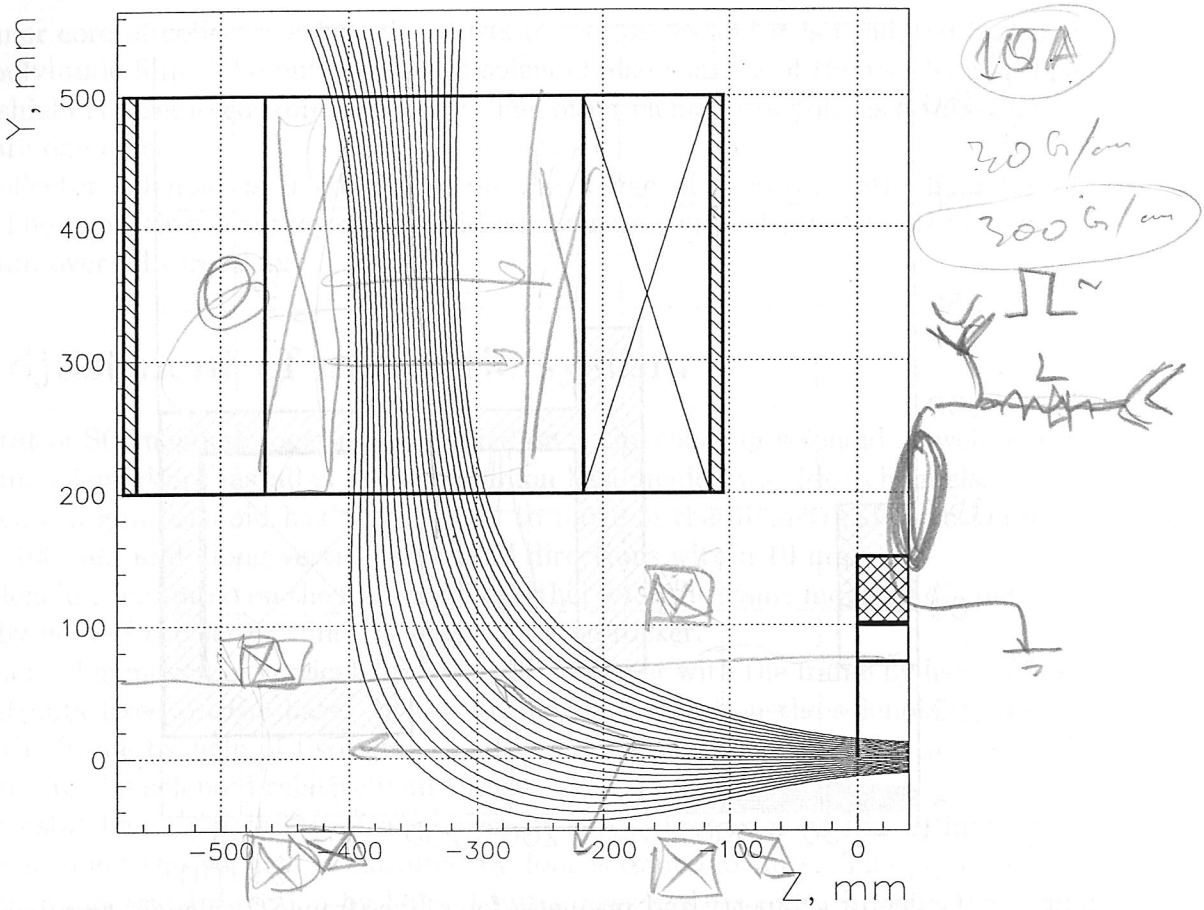

Figure 17: Magnetic force lines from electron gun solenoid to SC solenoid.

9.2 Collector solenoid

The collector geometry choice was found the most complicated stage in optimization of all geometry of TEL. There were some reasons explaining this trouble:

- dimensions of collector were unknown and they were changed several times in side of increase;
- the design of collector also was changed several times: collector with shelf and without one and so on;
- the distance from SC solenoid to collector was varied;
- the other parameters were also as a variation: thicknesses of iron walls, the number of turns, radii of covers etc.

After completion of overall calculations, the geometry of collector, which satisfies all conditions, was chosen and it is shown on Fig.18 together with magnetic force lines.

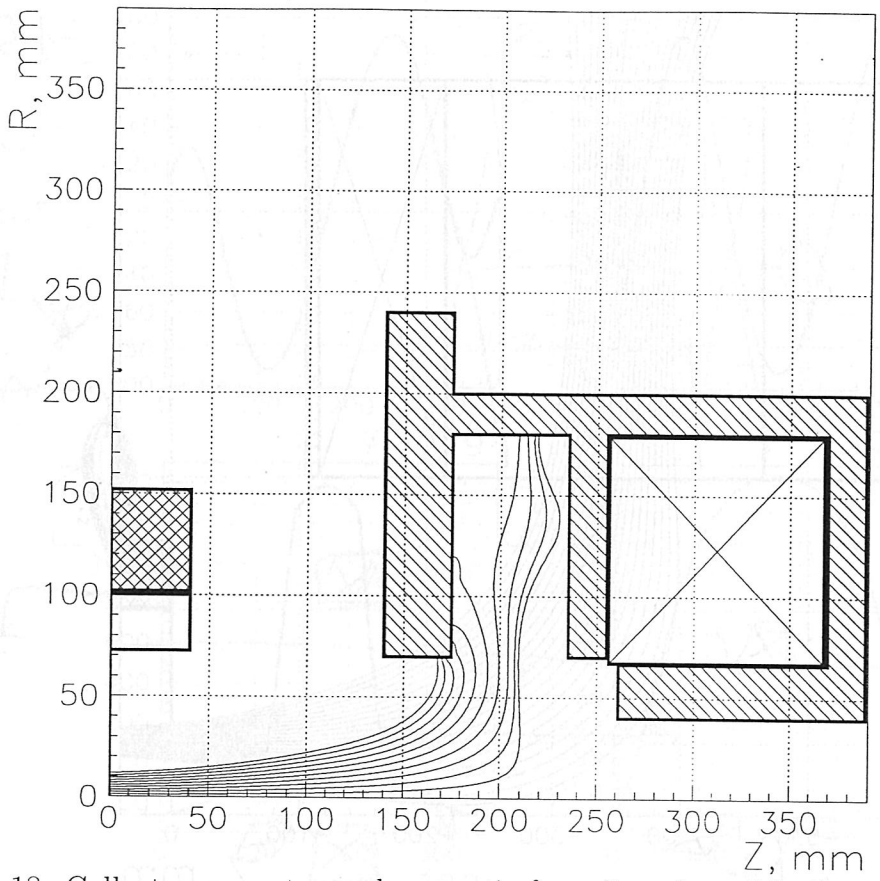

Figure 18: Collector geometry and magnetic force lines from SC solenoid to collector.

The main parameters of the collector solenoid are presented in Table 17.

Table 17: Main parameters of collector solenoid.

Inner radius, mm	67.4
Outer radius, mm	179.0
Length, mm	111.6
Total current, kA	-12.24
Turn number	$144 = 12 \times 12$
Maximal operating current, A	-85
Number of cooling circuits	1
Water flow, g/s	2.2
$\Delta T, ^\circ C$	30
Water Δp, atm	0.5

The coil consists of six flat two–row coils connected together successively by soldering of silver solder. Each of coils is impregnated by special compound on the base of epoxy resin.

The inner core of collector solenoid consists of two pieces and it is insulated by three layers of polyimide film. The outer flange of solenoid also consists of the two leaves. The magnetic shield is assembled from four parts. The other elements of yoke as a tube, flange and ring are one-piece.

The collector solenoid is fixed rigidly on the flange of cryostat with diameter of 430 mm. The expecting accuracy of solenoid adjustment relatively cryostat is not worse then 0.5 mm over all directions.

10 Adjustment of magnetic system

The cryostat of SC magnets together with fixed on it the collector solenoid as well as the electron gun solenoid are installed on the common base made by welded channels.

The electron gun solenoid has a possibility to move in the diametrical direction over a range of 100 mm and along vertical and axial directions within 10 mm.

The solenoid is mounted on the frame and together with the frame moves in diametrical direction by help of the screw which is screwed in the rocker.

The solenoid is moved in vertical direction also together with the frame by help of four screws and nuts fixed on the base. In the longitudinal direction the solenoid is moved relatively the frame by help of two screws and nuts. The support system of the solenoid allows to rotate the solenoid relatively all three axes.

The cryostat has a possibility of displacement along three axes within 10 mm. The displacement along the vertical is executed by four screws and nuts. The cryostat can move in the diametrical direction by help of two screws and tie-rods. In axial direction the cryostat is moved by four screws. It is possible rotations relatively all three axes.

The adjustment of magnet position is performed with help of the reference points fixed on the electron gun solenoid and the cryostat. The location of solenoids is locked by wrapping of nuts.

11 Conclusion

The magnetic system of TEL has been developed and its detail drawings have been produced. The main parameters of design in general drawings are correspondence to Technical Specification. Some parameters were changed accordingly concordance with FNAL:

- main solenoid current is increased from 1200 to 1800 A;
- gun solenoid turn current is increased from 200 A to 350 A.

References

[1] V.Shiltsev. Beam-beam Compensation Using Electron Beam in Tevatron. HEACC'98. Dubna, 1998.

V.Shiltsev et al. Compensation of Beam-beam Effects in the Tevatron with Electron Beams. FNAL-Pub/98-260.

[2] L.M. Tkachenko, Code Package MULTIC for Calculation of Magnetic Field with an Arbitrary Configuration. Preprint IHEP 98–28, Protvino, 1998.

[3] V.I. Balbekov, L.M. Tkachenko, "Optimization of the end parts of the UNK SC–dipoles," Preprint IHEP 82–167, Serpukhov, 1982 (in Russian).

[4] A Report on the Design of the Fermi National Accelerator Laboratory Superconducting Accelerator. May, 1979, FNAL, Batavia, Illinois.

[5] R.Hanft et al. Magnetic Field Properties of Fermilab Energy Saver Dipoles. IEEE Trans. on Nuclear Science. Vol.NS-30, No.4, August, 1983, p.p.3381-3383.

[6] S.V. Purtov, L.M. Tkachenko, "HARM–3D — a Code to Calculate Magnetic Characteristics of Superconducting Magnets," Proc. of XV Conf. on Magnet Technology, Bejing, China, 1997.

[7] V.I. Balbekov et al. Magnetic Field Quality in the Pilot Industrial Batch's SC Dipoles for the UNK. IPAC'92, Hamburg, 1992.

[8] Alexandrov A.G. et al. Automatic Measuring System for Superconducting Wires Parameters. IHEP Preprint 87-197. Serpukhov, 1987.

[9] Baidakov A.N. et al. Low Temperature Study of Magnetic Properties of Stainless and Electrical Steel for UNK SC-Magnets. IHEP Preprint 92-77. Protvino, 1992.

[10] Krivolutskaya N.V. and Rusinov A.I. Calculation of mechanical stresses in solenoid with compaund material with taken into account preliminary tension of turns. Works of Physical Institute of Russian Academy, 1980, V121, p.p15–51.

[11] Kozub S.S., Zubko V.V. Mechanical and Thermal Properties of Structural Materials and Coil of UNK Superconducting Magnet. Proc. of MT15, Beijing, 1998, p.p.1186-1189.